Green Synthesis of Graphene Oxide Flakes and Foams directly from Table Sugar

Majid S. Al-Ruqeishi[1*], Tariq Mohiuddin [2*], Noora Al-Ghafri[2]

1*. Physics Section, Department of Mathematical and Physical Sciences, College of Arts and Sciences, University of Nizwa, P.O. Box 33, P.C. 616, Barakit Al-Mouz, Nizwa, Sultanate of Oman

2*. Department of Physics, College of Science, Sultan Qaboos University, P.O. Box 36 P.C. 123, Al-Khoudh, Sultanate of Oman.

*Corresponding authors Emails: majiduon@unizwa.edu.om and tariqm@squ.edu.om

Abstract: Large scale of graphene oxide (GO) sheets and three-dimensional foams were fabricated directly from table sugar solution (TS) without using blowing agents. Using table sugar or biomass-derived carbohydrates as precursors provides a green, safe, and potentially scalable route for graphene oxide synthesis. These carbohydrate-based methods minimize hazardous reagents and waste through simple thermal decomposition processes. Compared to conventional techniques, they offer lower costs, fewer chemical risks, and greater sustainability, making them suitable for industrial applications. The use of catalytic carbonization (CC) on copper foil as well as non-catalytic (NC) hydrothermal carbonization in a sealed container produces separate GO sheets with 2.5 ± 0.1 cm in size. Non-catalytic growth produced GO 3-D foams with surface area ~7.5 ± 0.1 cm² and average grain sizes (7.97 ± 0.01 μm) comprising of 75.7% and 24.3% of carbon and oxygen respectively. HRTEM and SAED confirmed its hexagonal structure formation. After synthesis by graphitization, foams showed diminished groups containing oxygenated functionalities and C/O ratio increased from 0.13 to 1.5 as per XPS and FTIR results. On the other hand, 3D conductivity of the reduced GO or rGO increased by 0.87Ωm^{-1} compared to 0.04 Ωm^{-1} for GO. The present eco-friendly method offers scalability towards high-quality production of both GO and rGO for various applications.

Key words: Graphene, Graphene Oxide, reduced Graphene Oxide, Chemical vapor depositionn.

1. Introduction

Graphene with an extraordinary electronic and mechanical properties, attract many researchers and give rise to a variety of applications (Aïssa, Memon, Ali, & Khraisheh, 2015; Bae, Kim, Shin, Ahn, & Hong, 2012; Novoselov & Geim, 2007; Partoens & Peeters, 2006). Exfoliation of high oriented pyrolytic graphite (HOPG) considered as the main process to appeal off graphene sheets out of graphite stacks in agitative liquid medium (Hernandez, Lotya, Rickard, Bergin, & Coleman, 2010; Stankovich et al., 2006). Other studies implemented laser (Chyan et al., 2018) and MnO2 in Hummer's method (Sujiono et al., 2020) to end with floating graphene layers. Furthermore, when it comes to the high quality and low scalability, CVD method was chosen as favorable method (Kim et al., 2011; Xuesong Li et al., 2009; Reina et al., 2009). In conventional Graphene CVD growth process depends on pure Cu and Ni substrates and highly purified methane and hydrogen gases under high vacuum and temperature with controllable cooling, heating and gas flow rates systems.

On the other hand, green synthesis of graphene and graphene oxide by a direct thermal heating of row sources of carbon like saccharose and other natural sugars were utilized. In CVD, the

fabrication is preferred on catalyst like copper substrates at temperature range 1000-1050 °C (Ruan, Sun, Peng, & Tour, 2011). The use of polycrystalline copper foil as a substrate is widespread due to its low carbon solubility, which limits carbon precipitation and thus favors the growth of predominantly monolayer graphene (Li et al., 2009). In addition, for non-sugar sources such as PMMA (Byun et al., 2011), Polystyrene (Wu et al., 2013), flower petals (Ray et al., 2012), sugar-urea (Pan, Jin, Fu, Liu, & Zhang, 2013), graphitized anthracite coal (Zhou et al., 2012), plastic (Sharma et al., 2014), coconut shell waste (Sujiono et al., 2020), cookies and chocolate (Yan et al., 2011) were investigated as a good alternative sources with more modifications. This self-limiting behavior is critical for achieving high-quality graphene films, as confirmed by numerous studies utilizing both conventional thermal chemical vapor deposition (CVD) and more advanced methods (Li et al., 2009). Electromagnetic induction heating further enhances process efficiency and graphene quality by rapidly achieving the target temperature and minimizing defect density (Byun et al., 2011). The geometry of the copper substrate, reaction conditions, and the concentration of source precursors all influence the quality and coverage of the resulting graphene. The sugar sucrose melts at 186°C and undergoes thermal decomposition. The sucrose breaks down through dehydration, releasing water vapor and leaving behind carbon. This carbonizing process produces a carbon-rich residue due to the absence of expansion, typical of reactions with blowing agents like sodium bicarbonate. This represents pyrolysis, where organic compounds decompose at high temperatures short of oxygen or catalysts (Wang et al., 2017). During heating, the byproduct gaseous are released, including water vapor (160–190°C), carbon dioxide (CO_2) (after 190°C), and carbon monoxide (CO) (above 250°C) under oxygen-limited conditions. Between 200°C and 350°C, volatile organic compounds such as acetic acid, acetone, and aldehydes are emitted, contributing to the burnt odor. At temperatures above 350°C, thermal cracking produces light hydrocarbons like methane (CH_4), marking the progressive breakdown of sugar during pyrolysis (Shafizadeh, 1982; Tomasik et al., 1989). When the temperature rises to near 1000°C, methane (CH_4) and hydrogen (H_2) are produced, which can serve as precursors for graphene production via thermal chemical vapor deposition (CVD). In this process, methane acts as a carbon source, while hydrogen helps foster monolayer graphene growth and controls the size and morphology of graphene films. Hydrogen also assists in reducing carbon species, safeguarding the formation of high-quality graphene (Shafizadeh, 1982). Recent studies show that methane developed from biomass, including sugar pyrolysis, can be effectively used in thermal CVD to produce graphene. This process promotes from the methane and hydrogen produced during pyrolysis, contributing to a green, carbon-negative

approach for large-scale graphene production (Hernández et al., 2022; Nam et al., 2024).

Using table sugar (sucrose) or biomass-derived carbohydrates as precursors offers a greener, safer, and potentially scalable alternative to conventional oxidative methods of graphene oxide (GO) synthesis. For example, recent work demonstrated that simple pyrolysis of sugarcane leaves produces high-quality GO with minimal hazardous reagents and reduced waste (Thangaraj et al., 2023). Similarly, employing commercial sugar in templated pyrolytic processes yielded porous carbon materials with GO-like structures via an inexpensive, low-risk procedure easily adaptable to industry (Besinella et al., 2021). Compared to standard methods, these carbohydrate-based routes avoid strong oxidizers, reduce chemical hazards, and leverage low-cost, abundant feedstocks, highlighting their scalability and sustainability.

In this study is focused on 3-D GO foam and 2-D GO sheets fabrication directly from table sucrose C12H22O11 without the use of blowing agents. The synthesis involved in two hydrothermal carbonization processes, (1) catalytic carbonization (CC) growth of GO on copper foil and (2) non-catalytic synthesis growth by heating the TS solution inside closed container at controlled parameters.

1. Experimental setup

GO sheets and 3D foams were fabricated by a direct heating of table sugar solution (TS), NAKHAH sugar brand from Family Food Manufacturing and Packaging Company. The TS solution was prepared by mixing and sonicating 1-18 g of TS, sucrose C12H22O11, which consist of glucose and fructose, with 50 ml of DI water as shown in table1, to undergo catalytic and non-catalytic carbonization.

2. Catalytic Carbonization (CC)

A mixture of TS solution is added into a cleaned ceramic boat, which is fully covered and mounted with copper foil. The copper foil (Jans Copper Co.) is a single side treated electro-deposited finish 99.99% with 0.1 mm thick that comes with enhanced high temperature elongation properties, high thermal stability and high resistance to oxidation. The sugar-filled copper-covered boat is centered inside a quartz tube, which placed in a horizontal furnace as shown in Fig1 (C1). Then the quartz tube is vacuumed, 10-4 mbar, and hence, Ar gas is introduced and kept at 100 sccm flowrate. After that, the temperature was raised up to 800˚C with steady heating rate of 1.5 C/s for 30 minutes. Finally, the system was cooled down naturally and the samples labeled GO-1 were removed for further characterizations.

Table 1. Concentration values of prepared sugar solutions

Sugar Mass m±0.05(g)	Water Volume V±0.5 (ml)	Concentration C±1.05 (g/ml)
18.00	50.0	0.36
16.00	50.0	0.32
12.00	50.0	0.24
10.00	50.0	0.2
9.00	50.0	0.18
6.00	50.0	0.12
3.00	50.0	0.06
1.00	50.0	0.02

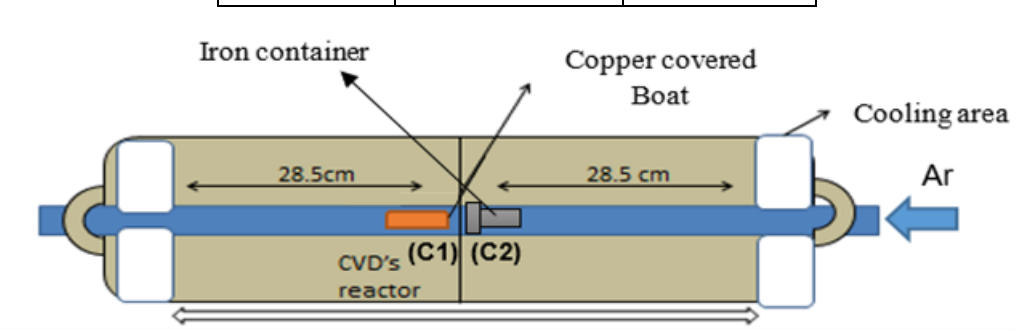

Figure 1. Experimental setup for the catalytic and non-catalytic growth of GO.

3. Non-catalytic Growth (NC)

The TS solution was placed inside a closed and sealed iron container, designed to work under high pressure and temperature as shown in Fig.1 (C2). Then, the container was loaded into a middle of a quartz tube, which was mounted inside the horizontal furnace. The system was vacuumed and Ar gas was introduces at 100 sccm flowrate to eliminate unwanted gases. Then the furnace temperature was raised with 1.5C/s up to (160-175°C), as required, and then kept for 30 minutes. Finally, the resultant black solid spume or graphene oxide foam, and floated 2D material, GO-2 layers, were collected from the container at each experiment and kept dry after annealed for further characterizations. Products Morphology and structural analysis were conducted by field-emission scanning electron microscopy (FESEM), energy-dispersed X-ray spectroscopy (EDX), and transmission electron microscope (TEM). Optical analyzation was achieved by FTIR, and Raman spectroscopy.

4. Graphitization process (reduction of GO)

In this process, foam samples were heated up again up 1000C^{o} under argon atmosphere for two hours to get rid of the functional groups that affect the graphene foam properties. The air inside the tube furnace was evacuated using

suction bump into ventilation outlet system and then directly the argon gas was flushed inside the tube to provide suitable graphitization conditions by ensuring that it do not interact with the foam inside as shown in figure 1. This graphitization process production will be subjected for further characterizations to make sure that most of the surface functional groups over graphene foam were reduced or (RGO).

2. Results and discussions

1. Synthesis of GO sheets and foams.

In this study, both non-catalytic and catalytic processes were working to synthesize graphene group of chemical elements (GO) derivatives in the form of foams and sheets. The non-catalytic synthesis was achieved by thermally acting a TS resolution inside a sealed iron container, yielding two unconnected structural morphologies: three-dimensional (3D) foam-like structures and floating sheets, designated as GO-f and GO-1, respectively. The GO-f samples exhibit a black color, and a very interconnected structure composed of limited carbon spheres. Morphological analysis, as depicted in Fig. 2(a), reveals that the GO-f foam possesses a surface area of nearly 7.5 ± 0.1 cm². Further test through scanning electron microscopy (SEM), shown in Fig. 2(b-c), indicates that the grain sizes within the foam range from 3.41 to 12.50 ± 0.01 µm, indicating a heterogeneous microstructure. Elemental composition analysis via energy-dispersive X-ray spectroscopy (EDX), presented in Fig. 2(d), proves the presence of carbon and oxygen in the GO-f samples, with atomic percentages of 75.7% and 24.3%, respectively. This C/O ratio implies a moderate degree of oxidation, consistent with the structural characteristics of graphene oxide-based foams. These findings highlight the successful synthesis of GO derivatives with distinct morphologies and provide a foundation for further investigation into their physicochemical properties. On the other hand, floated GO-1 sheets were obtained on the surface of the sugar liquid solution. While, a small portion of contained sugar solution was leaked out from the closed iron container due to a high pressure and temperature conditions. GO-1 is found to be transparent ~ 79%, brownish in color with 2.5 ± 0.1cm in size as shown in Fig. 2(e). Because the main source of carbon is the sugar solution, the grown thin layer can be only attributed to the molten sugar solution, as it will be explained in the growth mechanism part. The images from HRTEM in Fig. 2(f) indicates the graphene oxide sheet hexagonal structure and the magnified lattice shown in Fig.2(g) reveals the stacks of GO layers, see the square region of Fig. 2(f). The darker parts of the HRTEM image in Fig. 2(f) represents folded sheets. Selected area electron diffraction (SAED) taking from both lighter and darker areas indicates the crystal orientation of the repeated hexagonal ring structure of GO single layer. GO surface is smooth with some pits or holes. Secondly, in the catalytic carbonization process the grown GO sheets, labeled GO-2, occur at the surface of the FCC copper foil. Here, the carbon atoms were

directly adsorb from the high heated and compressed vaporized sugar solution as it will be explain in the growth mechanism part. The HRTEM image of transferred GO-2 sample is revealed in Fig. 2 (h). The EDX reveal elemental composition before and after transferred from the Cu foil are shown Fig. 2(i) and (j) respectively. FTIR spectra in Fig. 3(a), illustrates the absorption bands related to vibrating functional groups attached to GO sample. The band centered at 3300 cm-1 is attributed to hydroxyl O-H stretching vibration of the C-OH group. C=C from unoxidized sp2 CC bonds is represented by the sharp band at 1650 cm-1 (Berciaud, Ryu, Brus, & Heinz, 2009). The band at 1180 cm-1 is assigned to C-O stretching vibration, and stretching vibration of C-O-C at 1055 cm-1 (Kudin et al., 2008). There was no band at ≈1570 cm−1 (i.e., no graphitic stretching vibrations), confirming the high quality of the GO samples.

Figure 3(b) shows room-temperature Raman spectrum in the wavenumber range of (250 – 1800) cm−1 for an excitation wavelength of 638 nm. G band and D band, the major Raman features of graphene oxide are centered at ~1592 cm-1 and ~1340 cm-1 respectively. The G band originates from in-plane vibration of sp2 carbon atoms is a doubly degenerate (TO and LO) phonon mode (E2g symmetry) at the Brillouin zone center (Phan, Vincent, Cherns, Nghia, & Ursaki, 2008) and the D band originates from a two phonon double resonance Raman process (Castiglioni, Tommasini, & Zerbi, 2004). It can be seen in Fig. 3 (b) that the D band becomes broader and blue-shifted for thicker graphene thickness, as seen in the GO-2 curve (Ferrari, 2007). Peaks at 521cm-1 and 943 cm-1 are attributed to the Si/SiO2 substrate.

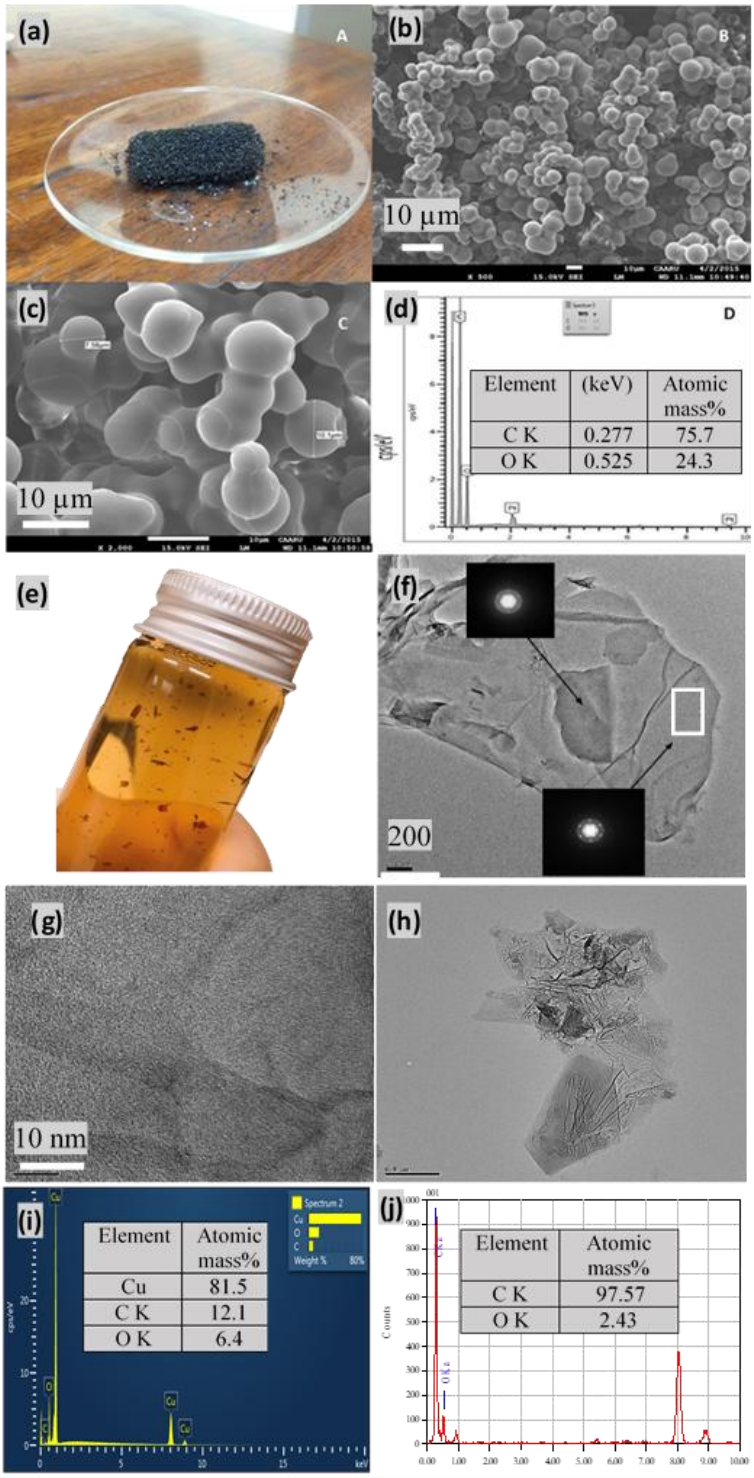

Figure (2): (a) photograph of carbon foam, (b-c) FESEM image carbon foam and it is related (d) EDX spectrum. (e) Photograph of GO-1 solution. (f) HRTEM image of GO-1 flakes with SAED spots taken from different areas, (g) HRTEM image of GO-1 stacks of layers in the white square region of (f). (h) HRTEM image of GO-2 and its (i) EDX spectrum before removed from Cu foil and (j) EDX result for transferred GO-2 layer.

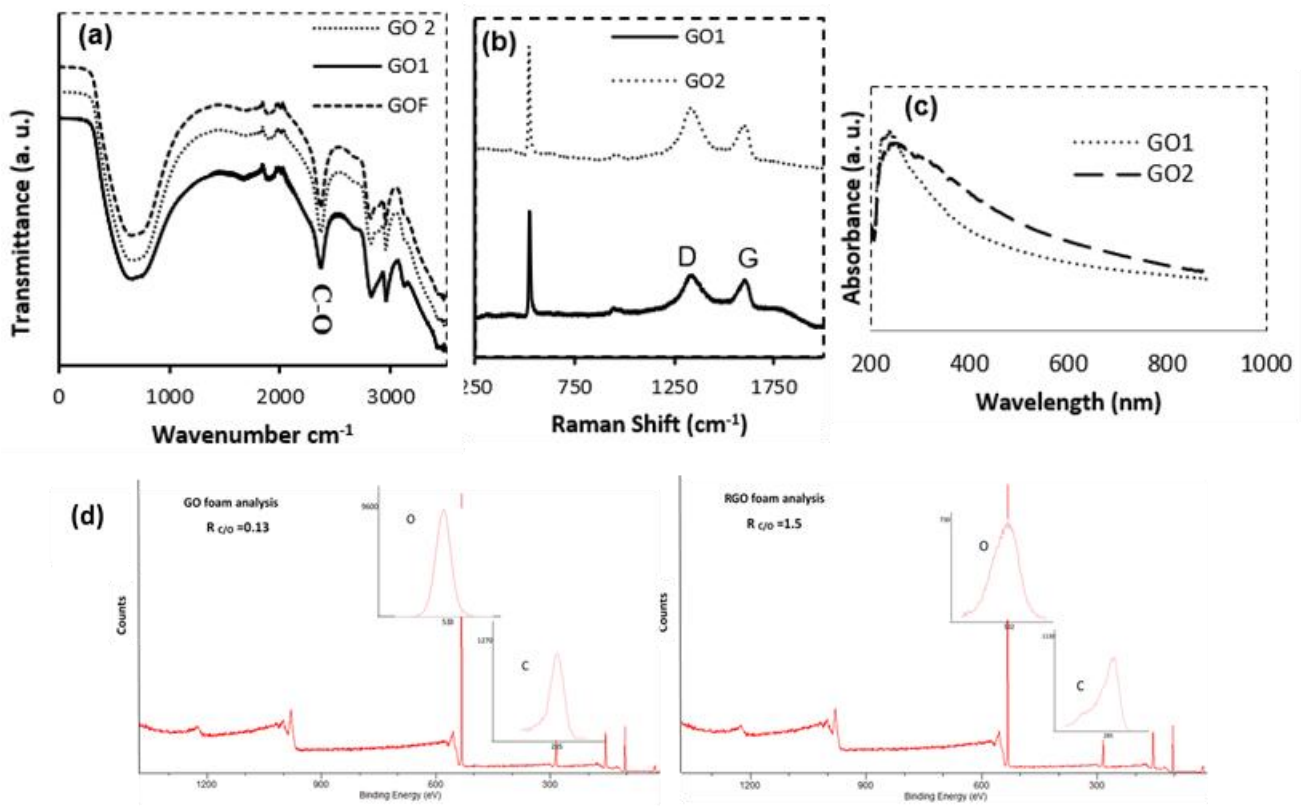

Figure 3. (a) Fourier-transform infrared spectra in transmittance mode taken from graphene oxide layers, GO-1, GO-2 and GOF. (b) The corresponding room-temperature Raman spectra and (c) UV-visible spectra of the as-synthesized graphene oxide for tow GO-1 and GO-2.(d) XPS spectra of GO and r-GO foams.

The UV–Vis spectra taken for 0.05 mg ml−1 water dispersed graphene oxide solutions, GO-1 and GO-2 methods; shows a peak centered at about 220–240 nm as revealed in Fig. 3(c). The spectrum of GO-2 sample has a main absorption peak at 229 nm and a shoulder peak at 290-300 nm, which are attributed to π-π* transition of C=C bonds(Peng et al., 2015). The optical absorption is changing with the number of layers, for a thicker GO layers (>10), the maximum adsorption band disappears and instead a lower wavelength of 196 nm is dominant as reported by (Luo, Lu, Somers, & Johnson, 2009). XPS spectra (fig. 3d) C 1s region for GO foam and r-GO foam indicate the chemical composition and bonding states. For GO foam, the deconvolution of spectrum C 1s results in three main peaks: ~284.5 eV(sp^2/sp^3 C-C/C=C), ~286.5 eV(C-O, epoxy/hydroxyl), and ~288.5 eV(C=O, carbonyl). The ratio of C/O is 0.13 indicates a high degree of oxidation which confirms FTIR results as well. In r-GO foam, the intensity of the peaks related to C-O and C=O has been reduced significantly with an increased C/O ratio of 1.5 that can be attributed to removal of oxygen containing functional groups incorporated during the synthesis process upon reduction away from itself rGO

conversion. Both binding energy shifts and peak intensities confirm the successful reduction of GO to rGO with restoration of some of the sp2 carbon network.

2. Graphene and Reduce Graphene Foams.

XPS spectra of GO and r-GO foams, shown in Fig. 3(d), were analyzed using CasaXPS software. GO and r-GO foams were tested. The observed peak positions and their related carbon functional groups are summarized in table 4 according to XPS library data (Jörgen Bergström, 2015).

Table 2. Peak positions of carbon functional groups.

Functional group	Peak position (eV)
Aromatic carbon (C-C sp2)	284.7
Aliphatic carbon (C-C sp3)	285.3
Hydroxyl (C-OH)	285.9
Epoxy (C-OC)	286.6
Carbonyl (C=O)	288.3
Carboxyl (O-C=O)	290.4

XPS technique was used to evaluate the percentage of oxygen in the samples by calculating carbon to oxygen atomic ratio (C/O) or R_{CO} from extracted sum spectra of carbon and oxygen as demonstrated in top of Fig4. The R_{CO} was calculated using equation 7 each time. Value of R_{CO} was approximately 1.5 and 0.13 for r-GO and GO foams respectively, concluding that the percentage of oxygenated groups was decreased with graphitization process.

GO and r-GO foams were studied by testing the conductivity of a selected area. Conductivity was calculated using the resistance of about 1×1×1 cm^3 of a cube after calculating the resistivity as mentioned in equations 1, 2.

Resistivity ρ can be calculated by:

$$\rho = \frac{R\,A}{L} \qquad (1)$$

Where R is the measured resistance from the cube using the digital multi-meter. Conductivity is the inverse of resistivity with the relation:

$$\sigma = \frac{1}{\rho} \qquad (2)$$

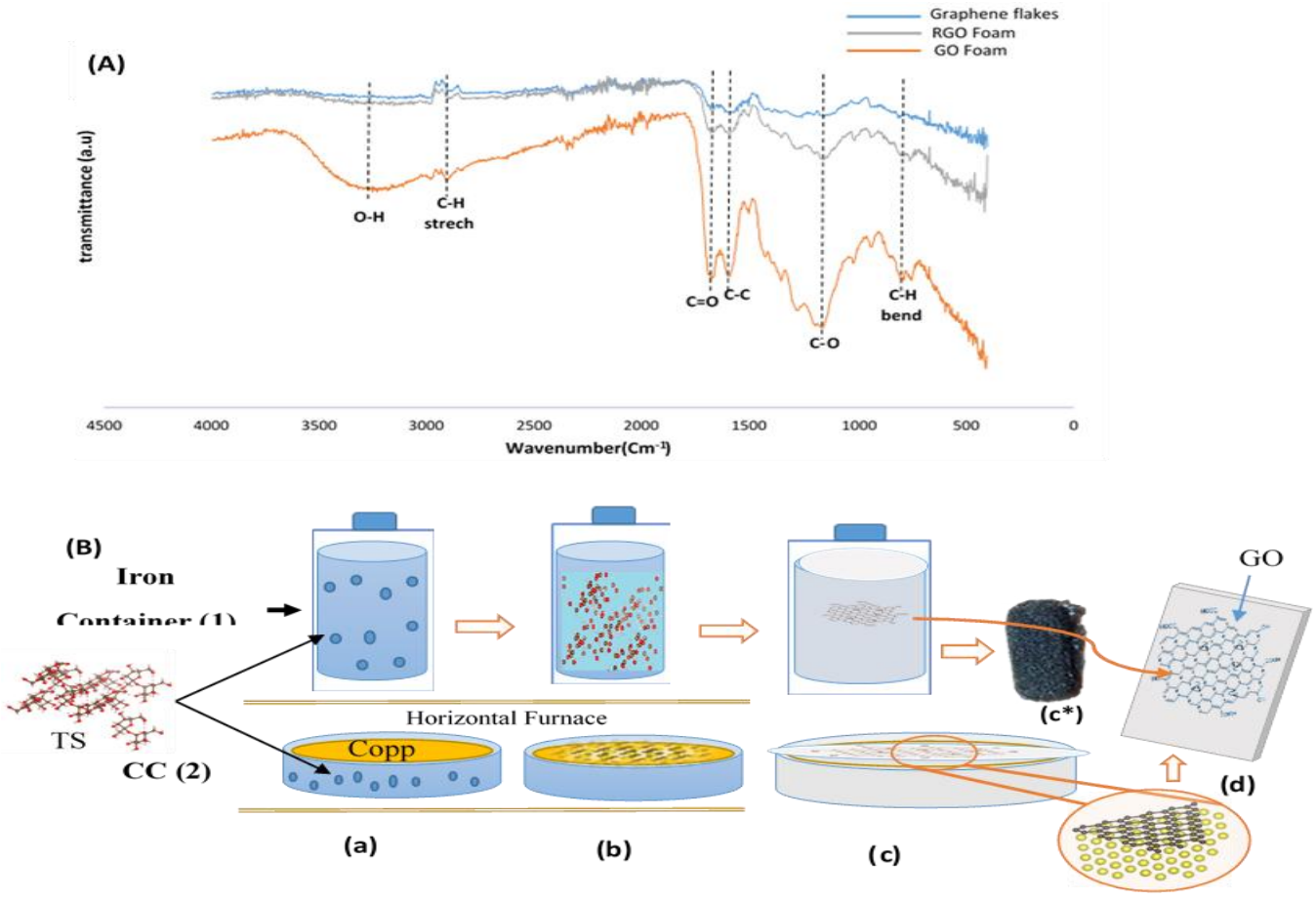

Figure 4. (A) FTIR spectra of GO flakes, GO and r-GO foams. (B) Schematic illustration of GO sheets and foam growth mechanisms. (a1&2) TS dissolved in DI water to obtain a colorless transparent

solution. (b1) Polymerized TS molecules start to assemble and nucleation inside the iron container. (c1) TS dehydrate intermolecularly to form a sheet of GO, which then floats on the surface of the solution. (d1) residuum of the black carbon foam under floated GO-1 (c1) within the iron container. (b2) in CC process the heated TS molten solution makes precursors like carbon, oxygen and hydrogen to transport and adsorb subsequently into the lower Cu substrate and form (c2) GO-2 layer in the CC process. (d1 and d2) The as-grown GO layers are transferred into silicon substrate by dipping and lifting form both methods.

The different measured resistances and their corresponding resistivity and conductivity are listed in Table 3. The average conductivity of GO foam cube was about 0.04 Ωm-1, where average conductivity of r-GO foam was around 0.87 Ωm-1. Unfortunately, the accepted conductivity of single layer graphene could not be obtained exactly. Nevertheless, the conductivity of the graphitized foam was much higher than the normal one. The increasing in conductivity level indicates that the purpose of graphitization process was achieved by eliminated many bonded functional groups.

Table 3. Measured resistance and their corresponding resistivity and conductivity.

Sample	R ±10 (Ω)	ρ ±0.20 (Ωm)	σ±0.01 (Ωm^{-1})
GO foam	15000	15.00	0.07
	30000	32.00	0.03
	100000	100.00	0.02
r-GO foam	2000	2.00	0.50
	700	0.70	1.43
	2000	1.50	0.67

Concentration of 0.24 g/ml reaching the target temperature 180C^{o} under heating rate of (0.35 C^{o}/s) produced a good GO foam that goes under graphitization process to reduce graphene oxide, or to form r-GO. FTIR spectra shown in Fig4 (A). reveals less functional groups for r-GO comparing of both GO flakes and foams. This is due to reduction in transmittance bends of oxygenated functional groups. The r-GO foam was demonstrated as near form of graphene with close features.

3. Growth mechanism

Non-Catalytic Growth

In Fig. 4(B: a-d) a schematic illustration shows the steps of GO sheet and foam growth mechanisms. Fig. 4 (B: a1-d1) illustrates the non-catalytic growth of GO-1 by direct heating of dissolved TS in DI water to obtain a colorless transparent solution. TS contains -OH, -CH2OH, and –C–O–C– functional groups. The heating process at (175 ± 2 °C), within 30 minutes, makes these functional groups undergoes covalent cross-linking reactions. This will form C–C and C=C bonds through the removal of water and CO2. This polymerization process of TS starts under hydrothermal conditions as shown in Fig. 4 (B: a1 and b1). As a result, the molecules dehydrate intermolecularly to form the first seeds or nucleation sites of 2D of honeycomb network, which evolve into GO layer as revealed in Fig. 4 (B: c1). The formed floated layer get thicker as it adsorb more carbon atoms. Then, when system is cooled down, the GO-1 layer floats onto the surface of the solution due to its hydrophobic nature of the GO layer. Subsequently, it is transferred onto silicon substrate by dipping and lifting. The transferred GO sheets is rinsed by dipping into DI water to remove the residues and then annealed at 150 ^{o}C to dehydrate and graphitize for tuning its structural and optical properties.

At the same time the remaining seeding carbon atoms form a network in 3 dimension. This formation left vacancies due to the high pressure dynamic motion and the solidification rate of the sugar solution. Sequentially, porous 3D foam produced until the carbon feed stock vanished. One example of the produced foams is revealed in Fig. 4(B: c*).

Catalytic Carbonization (CC).

Graphene oxide (GO) was synthesized using the Catalytic Carbonization (CC) method, and the complete mechanism is shown in Fig. 4(B: a2-d2). In this approach, a molten solution acts as a precursor source, releasing volatile species like carbon, oxygen, and hydrogen in a semi-enclosed environment. The precursors are then transferred to the back of a copper substrate, where the synthesis process begins. The copper substrate acts as a catalytic surface, enabling carbon atom adsorption. Once adsorbed, these carbon atoms disperse across the substrate surface, generating stable nuclei that serve as nucleation and subsequent growth sites for graphene layers, as shown in the schematic

illustration of the heating process in Fig. 4 (B: a2, b2, and c2).

Under specific conditions, gas-phase reactions may also occur, contributing to the complexity of the growth dynamics. As the process progresses, more carbon atoms are drawn from the solution-gas phase medium and move toward the substrate surface. This migration causes the buildup of carbon atoms, which eventually condense to form an extensive network of graphene layers at various sites on the substrate. Over time, these isolated networks join, forming a continuous graphene layer. Because of the presence of hydrothermal gases in the reaction environment, the as-formed graphene layer oxidizes, integrating a variety of oxygen-containing functional groups to produce graphene oxide (GO-2). The successful synthesis of GO-2 using this catalytic process demonstrates the importance of the copper substrate in encouraging carbon adsorption and nucleation, as well as the effect of the semi-enclosed environment on diffusion and oxidation processes. The addition of oxygen-containing functional groups, such as hydroxyl, epoxy, and carbonyl groups, during the oxidation process is compatible with the normal chemical composition of graphene oxide, as established by previous research on GO synthesis under hydrothermal conditions. This oxidation step is most likely caused by the graphene layer's interaction with reactive oxygen and hydrogen species found in hydrothermal gasses produced during the decomposition of the molten solution.

The CC method offers quite a few advantages for GO synthesis, including the ability to control the nucleation and growth of graphene layers through the catalytic activity of the copper substrate. However, the existence of gas-phase reactions introduces minor changes in the process, which may affect the uniformity and degree of oxidation of the resulting GO-2. This means that the chemical properties like (basal and edge oxygen functional groups, hydrophobicity, acidity (edge groups like –COOH) and electrical conductivity can be adjusted based on the gas-phase control(Kulyk et al., 2022). The heterogeneity in the graphene network formation, as observed in Fig. 4(B:d2), suggests that the growth conditions, such as temperature, precursor concentration, and reaction time, plays also a significant role in determining the final structure and properties of the GO layers. For example, higher temperatures may improve the diffusion rate of carbon atoms, leading to speedup network formation, while continued exposure to gas reactant could increase the degree of oxidation, potentially altering the electronic and chemical properties of GO sheets (Fang et al., 2016).

The presence of oxygen-containing functional groups in GO-2 may also introduce defects in the graphene lattice, as evidenced by the structural disorder typically observed in Raman spectra of GO (e.g., Fig. 3b from prior analysis). While oxygen presence will enhance

its solubility and reactivity and this can be modified to tailor the properties of GO sheets for specific applications. Generally, the CC process gives a viable route for the GO fabrication with the copper substrate. Also, the hydrothermal environment plays an important role in the nucleation, growth, and oxidation synthesis steps. These results confirm the vital role of reaction conditions in controlling the structural and chemical properties of GO sheets.

3. Conclusion

Graphene oxide sheets and foams were synthesized from sugar using direct catalytic and non-catalytic methods, providing a sustainable, low-cost alternative method to synthesized graphene. Catalytic carbonization yielded GO sheets on copper foil; the former yielded 3D foams (surface area ~7.5 ± 0.1 cm^2; grain sizes 3.41–12.50 ± 0.01 μm) that were ~75% carbon and ~24% oxygen, and the latter yielded sheets of GO-1 floating on water (approximately 79% transparent). HRTEM and SAED confirmed the hexagonal structure of the graphene oxide sheets with smooth surfaces having minor defects. Graphitization greatly reduced oxygenated functional groups (C/O ratio increase from 0.13 to 1.5 as per XPS and FTIR), hence increasing conductivity in rGO foam samples (0.87 Ω m^{-1} compared to ~0.04 Ω m^{-1} for foamed GO samples). Such results place table sugar as a feasible carbon source towards quality derivatives of graphene, thus opening up scalable green production for advanced material applications.

4. Acknowledgments

This research was funded by the Ministry of Higher Education, Research and Innovation, Sultanate of Oman, Grant (No. BFP/RGP/EI/24/014). The authors express their sincere gratitude for the ongoing support and encouragement from the University of Nizwa administration, which greatly facilitated this study. The authors also acknowledge the support provided by the SQU Strategic Grant (No. SR/SCI/PHYS/18/01). Furthermore, the authors extend their appreciation to Mr. Khamis Omair AL-Riyami from the DARIS Center for Scientific Research and Technological Development, University of Nizwa, SQU CAARU, and Dr. Myo Tay Zar Myint from the Surface Science Laboratory, College of Science, Sultan Qaboos University, for their valuable contributions to this research.

References

[1] Aïssa, B., Memon, N. K., Ali, A., & Khraisheh, M. K. (2015). Recent Progress in the Growth and Applications of Graphene as a Smart Material: A Review. Frontiers in Materials, 2(58). doi:10.3389/fmats.2015.00058

[2] Bae, S., Kim, S. J., Shin, D., Ahn, J.-H., & Hong, B. H. (2012). Towards industrial applications of graphene electrodes. Physica Scripta, 2012(T146), 014024.

[3] Berciaud, S., Ryu, S., Brus, L. E., & Heinz, T. F. (2009). Probing the intrinsic properties of exfoliated graphene: Raman spectroscopy of free-standing monolayers.

Nano Lett, 9(1), 346-352. doi:10.1021/nl8031444

[4] Byun, S.-J., Lim, H., Shin, G.-Y., Han, T.-H., Oh, S. H., Ahn, J.-H., . . . Lee, T.-W. (2011). Graphenes converted from polymers. The Journal of Physical Chemistry Letters, 2(5), 493-497.

[5] Castiglioni, C., Tommasini, M., & Zerbi, G. (2004). Raman spectroscopy of polyconjugated molecules and materials: confinement effect in one and two dimensions. Philos Trans A Math Phys Eng Sci, 362(1824), 2425-2459. doi:10.1098/rsta.2004.1448

[6] Chyan, Y., Ye, R., Li, Y., Singh, S. P., Arnusch, C. J., & Tour, J. M. (2018). Laser-induced graphene by multiple lasing: toward electronics on cloth, paper, and food. ACS nano, 12(3), 2176-2183.

[7] Hernandez, Y., Lotya, M., Rickard, D., Bergin, S. D., & Coleman, J. N. (2010). Measurement of multicomponent solubility parameters for graphene facilitates solvent discovery. Langmuir, 26(5), 3208-3213.

[8] Kim, J., Ishihara, M., Koga, Y., Tsugawa, K., Hasegawa, M., & Iijima, S. (2011). Low-temperature synthesis of large-area graphene-based transparent conductive films using surface wave plasma chemical vapor deposition. Applied physics letters, 98(9), 091502.

[9] Kudin, K. N., Ozbas, B., Schniepp, H. C., Prud'homme, R. K., Aksay, I. A., & Car, R. (2008). Raman spectra of graphite oxide and functionalized graphene sheets. Nano Lett, 8(1), 36-41. doi:10.1021/nl071822y

[10] Li, X., Cai, W., An, J., Kim, S., Nah, J., Yang, D., . . . Tutuc, E. (2009). Large-area synthesis of high-quality and uniform graphene films on copper foils. Science, 324(5932), 1312-1314.

[11] Li, X., Cai, W., An, J., Kim, S., Nah, J., Yang, D., . . . Ruoff, R. S. (2009). Large-area synthesis of high-quality and uniform graphene films on copper foils. Science, 324(5932), 1312-1314. doi:10.1126/science.1171245

[12] Luo, Z., Lu, Y., Somers, L. A., & Johnson, A. T. (2009). High yield preparation of macroscopic graphene oxide membranes. J Am Chem Soc, 131(3), 898-899. doi:10.1021/ja807934n

[13] Novoselov, K. S., & Geim, A. (2007). The rise of graphene. Nat. Mater, 6(3), 183-191.

[14] Pan, F., Jin, J., Fu, X., Liu, Q., & Zhang, J. (2013). Advanced oxygen reduction electrocatalyst based on nitrogen-doped graphene derived from edible sugar and urea. ACS applied materials & interfaces, 5(21), 11108-11114.

[15] Partoens, B., & Peeters, F. (2006). From graphene to graphite: Electronic structure around the K point. Physical Review B, 74(7), 075404.

[16] Peng, L., Xu, Z., Liu, Z., Wei, Y., Sun, H., Li, Z., . . . Gao, C. (2015). An iron-based green approach to 1-h production of single-layer graphene oxide. Nat Commun, 6, 5716. doi:10.1038/ncomms6716

[17] Phan, T. L., Vincent, R., Cherns, D., Nghia, N. X., & Ursaki, V. V. (2008). Raman scattering in Me-doped ZnO nanorods (Me = Mn, Co, Cu and Ni) prepared by thermal diffusion. Nanotechnology, 19(47), 475702. doi:10.1088/0957-4484/19/47/475702

[18] Ray, A. K., Sahu, R. K., Rajinikanth, V., Bapari, H., Ghosh, M., & Paul, P. (2012). Preparation and characterization of graphene and Ni-decorated graphene using flower petals as the precursor material. Carbon, 50(11), 4123-4129.

[19] Reina, A., Thiele, S., Jia, X., Bhaviripudi, S., Dresselhaus, M. S., Schaefer, J. A., & Kong, J. (2009). Growth of large-area single-and bi-layer graphene by controlled carbon precipitation on

polycrystalline Ni surfaces. Nano Research, 2(6), 509-516.

[20] Ruan, G., Sun, Z., Peng, Z., & Tour, J. M. (2011). Growth of graphene from food, insects, and waste. ACS nano, 5(9), 7601-7607.

[21] Sharma, S., Kalita, G., Hirano, R., Shinde, S. M., Papon, R., Ohtani, H., & Tanemura, M. (2014). Synthesis of graphene crystals from solid waste plastic by chemical vapor deposition. Carbon, 72, 66-73.

[22] Stankovich, S., Dikin, D. A., Dommett, G. H., Kohlhaas, K. M., Zimney, E. J., Stach, E. A., . . . Ruoff, R. S. (2006). Graphene-based composite materials. nature, 442(7100), 282-286.

[23] Sujiono, E. H., Zurnansyah, Zabrian, D., Dahlan, M. Y., Amin, B. D., Samnur, & Agus, J. (2020). Graphene oxide based coconut shell waste: synthesis by modified Hummers method and characterization. Heliyon, 6(8), e04568. doi:10.1016/j.heliyon.2020.e04568

[24] Wu, T., Ding, G., Shen, H., Wang, H., Sun, L., Jiang, D., . . . Jiang, M. (2013). Triggering the continuous growth of graphene toward millimeter-sized grains. Advanced Functional Materials, 23(2), 198-203.

[25] Yan, Z., Peng, Z., Sun, Z., Yao, J., Zhu, Y., Liu, Z., . . . Tour, J. M. (2011). Growth of bilayer graphene on insulating substrates. ACS nano, 5(10), 8187-8192.

[26] Zhou, Q., Zhao, Z., Zhang, Y., Meng, B., Zhou, A., & Qiu, J. (2012). Graphene sheets from graphitized anthracite coal: preparation, decoration, and application. Energy & fuels, 26(8), 5186-5192.

[27] Besinella, G. B., Padilha, J. E., Scheufele, F. B., Gasparrini, L. J., Borba, C. E., & Alves, H. J. (2021). Green synthesis of templated carbon porous materials from simple raw materials. Materials Advances, 2(1), 403–412. https://doi.org/10.1039/D0MA00483A

[28] Byun, S. J., Lim, H., Shin, G. Y., Han, T. H., Oh, S. H., Ahn, J. H., Choi, H. C., & Lee, T. W. (2011). Graphenes converted from polymers. Journal of Physical Chemistry Letters, 2(5), 493–497. https://doi.org/10.1021/JZ200001G

[29] Fang, L., Yuan, W., Wang, B., & Xiong, Y. (2016). Growth of graphene on Cu foils by microwave plasma chemical vapor deposition: The effect of in-situ hydrogen plasma post-treatment. Applied Surface Science, 383, 28–32. https://doi.org/10.1016/j.apsusc.2016.04.148

[30] Ferrari, A. C. (2007). Raman spectroscopy of graphene and graphite: Disorder, electron–phonon coupling, doping and nonadiabatic effects. Solid State Communications, 143(1–2), 47–57. https://doi.org/10.1016/J.SSC.2007.03.052

[31] Hernández, A. R. R., Cruz, A. G., Campos-Delgado, J., Hernández, A. R. R., Cruz, A. G., & Campos-Delgado, J. (2022). Chemical Vapor Deposition Synthesis of Graphene on Copper Foils. Graphene - A Wonder Material for Scientists and Engineers. https://doi.org/10.5772/INTECHOPEN.106058

[32] Kulyk, B., Freitas, M. A., Santos, N. F., Mohseni, F., Carvalho, A. F., Yasakau, K., Fernandes, A. J. S., Bernardes, A., Figueiredo, B., Silva, R., Tedim, J., & Costa, F. M. (2022). A critical review on the production and application of graphene and graphene-based materials in anti-corrosion coatings. Critical Reviews in Solid State and Materials Sciences, 47(3), 309–355. https://doi.org/10.1080/10408436.2021.1886046

[33] Li, X., Cai, W., An, J., Kim, S., Nah, J., Yang, D., Piner, R., Velamakanni, A., Jung, I., Tutuc, E., Banerjee, S. K., Colombo, L., & Ruoff, R. S. (2009). Large-area synthesis of high-quality and uniform graphene films on copper foils. Science, 324(5932), 1312–1314. https://doi.org/10.1126/SCIENCE.1171245/SUPPL_FILE/LI.SOM.PDF

[34] Nam, J., Yang, J., Zhao, Y., & Kim, K. S. (2024). Chemical vapor deposition of graphene and its characterizations and applications. Current Applied Physics, 61, 55–70. https://doi.org/10.1016/J.CAP.2024.02.010

[35] Shafizadeh, F. (1982). Introduction to pyrolysis of biomass. Journal of Analytical and Applied Pyrolysis, 3(4), 283–305. https://doi.org/10.1016/0165-2370(82)80017-X

[36] Thangaraj, B., Mumtaz, F., Abbas, Y., Anjum, D. H., Solomon, P. R., & Hassan, J. (2023). Synthesis of Graphene Oxide from Sugarcane Dry Leaves by Two-Stage Pyrolysis. Molecules, 28(8), 3329. https://doi.org/10.3390/MOLECULES28083329/S1

[37] Tomasik, P., Pałasiński, M., & Wiejak, S. (1989). The Thermal Decomposition of Carbohydrates. Part I. The Decomposition of Mono-, Di-, and Oligo-Saccharides. Advances in Carbohydrate Chemistry and Biochemistry, 47(C), 203–278. https://doi.org/10.1016/S0065-2318(08)60415-1

[38] Wang, W., Yang, S., & Wang, A. (2017). Observation of the unexpected morphology of graphene wrinkle on copper substrate. Scientific Reports, 7(1), 1–6. https://doi.org/10.1038/S41598-017-08159-8;TECHMETA=118,119;SUBJMETA=1053,301,357,639,918,925;KWRD=MECHANICAL+AND+STRUCTURAL+PROPERTIES+AND+DEVICES